NASA TN D-514

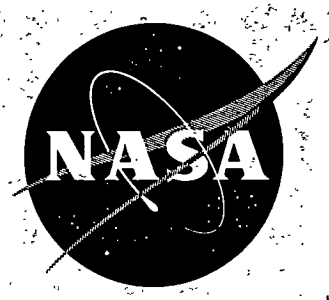

TECHNICAL NOTE
D-514

STATIC LONGITUDINAL STABILITY AND CONTROL CHARACTERISTICS AT A MACH NUMBER OF 1.99 OF A LENTICULAR-SHAPED REENTRY VEHICLE

By Charlie M. Jackson, Jr., and Roy V. Harris, Jr.

Langley Research Center
Langley Field, Va.

NATIONAL AERONAUTICS AND SPACE ADMINISTRATION
WASHINGTON

October 1960

NATIONAL AERONAUTICS AND SPACE ADMINISTRATION

TECHNICAL NOTE D-514

STATIC LONGITUDINAL STABILITY AND CONTROL CHARACTERISTICS AT A MACH NUMBER OF 1.99 OF A LENTICULAR-SHAPED REENTRY VEHICLE

By Charlie M. Jackson, Jr., and Roy V. Harris, Jr.

SUMMARY

An investigation has been made in the Langley 4- by 4-foot supersonic pressure tunnel at a Mach number of 1.99 to determine the longitudinal stability and control characteristics of a reentry model consisting of a lenticular-shaped body with two fin configurations (horizontal fins with end plates). Effects of deflecting the larger size fins as pitch-control surfaces were also investigated.

The results indicate that the body alone was unstable from an angle of attack of 0° to about 35° where it became stable and remained so to 90°. The addition of fins provided positive longitudinal stability throughout the angle-of-attack range and increased the lift-drag ratio of the configuration.

Reducing the horizontal-fin area at the inboard trailing edge of the fin had only a small effect on the aerodynamic characteristics of the vehicle for the condition of no fin deflection. Deflecting the fins appeared to be an effective means of pitch control and had only a small effect on lift-drag ratio.

INTRODUCTION

Several types of lifting reentry systems are currently under consideration. These include the system which utilizes small amounts of lift (ref. 1), modulated lift reentry (ref. 2), and high-angle-of-attack high-drag reentry (ref. 3). In the latter system the vehicle operates at a high angle of attack (near 90°) during the first portion of the reentry and, as the velocity decreases, an angle-of-attack transition occurs. The reentry is then completed with a gliding phase. A possible flight plan might require that the angle-of-attack transition occur in the supersonic speed range.

An investigation of the longitudinal aerodynamic characteristics of a proposed configuration being considered by the Space Task Group of the National Aeronautics and Space Administration for the high-angle-of-attack high-drag reentry was conducted in the Langley 4- by 4-foot supersonic pressure tunnel at a Mach number of 1.99. The configuration consisted of a lenticular-shaped body with movable fins (horizontal fins with end plates) to provide longitudinal stability and control through the transition and gliding phases of reentry. Tests were conducted through the angle-of-attack range from 0° to 90° with several control deflections. The results of these tests are presented herein without analysis.

SYMBOLS

All data are referred to the body-axis system except the lift and drag coefficients which are referred to the stability-axis system. The reference point for the pitching moment is located a distance of 45 percent of the body length rearward from the nose of the model. The coefficients are based on planform area and length of the body alone.

C_L	lift coefficient, $\frac{\text{Lift}}{qS}$
C_N	normal-force coefficient, $\frac{\text{Normal force}}{qS}$
C_D	drag coefficient, $\frac{\text{Drag}}{qS}$
C_A	axial-force coefficient, $\frac{\text{Axial force}}{qS}$
C_m	pitching-moment coefficient, $\frac{\text{Pitching moment}}{qSl}$
q	free-stream dynamic pressure, lb/sq ft
S	body planform area excluding fins, sq ft
l	body length, ft
M	free-stream Mach number
α	angle of attack, deg
δ	fin deflection, deg
L/D	lift-drag ratio

Subscripts:

b base

trim refers to a condition of longitudinal aerodynamic trim ($C_m = 0$)

MODEL AND APPARATUS

The model used in these tests consisted of a lenticular-shaped body with fins as shown in figure 1. Dimensions and details of the model are given in figure 2 and table I. The body shape was generated by revolving an ellipse with a major-to-minor-axis ratio of 2.73 about its minor axis. The fins and end plates had constant thickness (0.094 inch) and no camber. Tests were conducted for the conditions of fins off, basic fins with deflections, and modified fins (basic fins with the area reduced by a small triangular cutout at the inboard trailing edge) with no deflections. The fin deflection angle δ is taken as the rotary angle generated by the horizontal fin about its hinge line and is negative when the trailing edge of the fin is deflected upward. The end plates were rigidly attached to the horizontal fins so that the entire fin structure was deflected.

The model was supported in the tunnel by a sting system which permitted an angle-of-attack range from 0° to 90°. (See ref. 4.) Force and moment characteristics were obtained from a six-component strain-gage balance, and base pressures were obtained from a pressure tube located just inside the balance chamber of the model.

TESTS, CORRECTIONS, AND ACCURACY

The tests were conducted in the Langley 4- by 4-foot supersonic pressure tunnel with a Mach number 2.01 nozzle. Stagnation pressure was 6 pounds per square inch absolute and stagnation temperature was 100° F. The test-section Mach number for this pressure was determined by a previous calibration to be 1.99. The Reynolds number based on the body length was 0.988×10^6. In order to prevent condensation effects, the stagnation dewpoint was maintained at -25° F or below. Tests were made through the angle-of-attack range from 0° to 90° at zero sideslip.

The angles of attack were corrected for balance and sting deflections under load. The axial force, drag, and lift were corrected for

the condition of free-stream static pressure acting on the cross-sectional area of the balance chamber (referred to as base area). The axial-force coefficients due to the balance-chamber pressure are presented for each configuration tested. Unpublished data from sting-interference tests indicate that for angles of attack near 90° the effects of the model mounting system may introduce a probable error of 0.02 for the normal-force coefficient and 0.01 for the pitching-moment coefficient. The error for axial-force coefficient was not determined.

Estimated probable errors in force and moment data based on repeatability, zero shifts, calibration, and random instrument errors are as follows:

C_N	±0.002
C_A	±0.007
C_m	±0.004
$C_{A,b}$	±0.007
α, deg	±0.1
M	±0.01

PRESENTATION OF RESULTS

Selected schlieren photographs of the fin off, basic fin, and modified fin configurations are presented in figure 3. Other results of this investigation are presented in the following figures:

	Figure
Longitudinal aerodynamic characteristics of the model with fin off, basic fin, and modified fin configurations	4
Longitudinal aerodynamic characteristics of the model with basic fins at various fin deflection angles	5
Variation of $(L/D)_{trim}$ and $(C_L)_{trim}$ with α for the model with basic fins	6
Axial-force coefficients due to base pressures	7

SUMMARY OF RESULTS

The results of this investigation indicate that, with a moment center located at 45 percent of the body length, the body alone was unstable from an angle of attack of 0° to about 35° and then became stable and remained so up to 90°. The addition of the basic fins improved the static longitudinal stability to the extent that the configuration was stable throughout the angle-of-attack range. The lift-drag ratio was generally increased by the addition of the fins. Reducing the fin area at the inboard trailing edge of the fin (modified fin) had only a small effect on the aerodynamic characteristics of the vehicle. Deflecting the fins through a range from -30° to 20° as a pitch control was an effective means of controlling the vehicle through an angle-of-attack range from about -5° to 42°. This method of controlling results in a very small change in lift-drag ratio, the trimmed values of lift-drag ratio being essentially the same as the untrimmed values obtained with no deflection.

Langley Research Center,
National Aeronautics and Space Administration,
Langley Field, Va., June 23, 1960.

REFERENCES

1. Eggers, Alfred J., Jr., and Wong, Thomas J.: Re-Entry and Recovery of Near-Earth Satellites, With Particular Attention to a Manned Vehicle. NASA MEMO 10-2-58A, 1958.

2. Grant, Frederick C.: Importance of the Variation of Drag With Lift in Minimization of Satellite Entry Acceleration. NASA TN D-120, 1959.

3. Staff of Langley Flight Research Division (Compiled by Donald C. Cheatham): A Concept of a Manned Satellite Reentry Which Is Completed With a Glide Landing. NASA TM X-226, 1959.

4. Foster, Gerald V.: Exploratory Investigation at Mach Number of 2.01 of the Longitudinal Stability and Control Characteristics of a Winged Reentry Configuration. NASA TM X-178, 1959.

TABLE I

MODEL GEOMETRIC CHARACTERISTICS

Body:		
Length, in.		8
Base diameter, in.		1.25
Base area, sq in.		1.22
Planform area, sq ft		0.348
	Basic	Modified
Fins:		
Horizontal-fin area, sq in.	18.16	16.27
Vertical-fin area, sq in.	7.92	7.92
Leading-edge sweep, deg	10	10

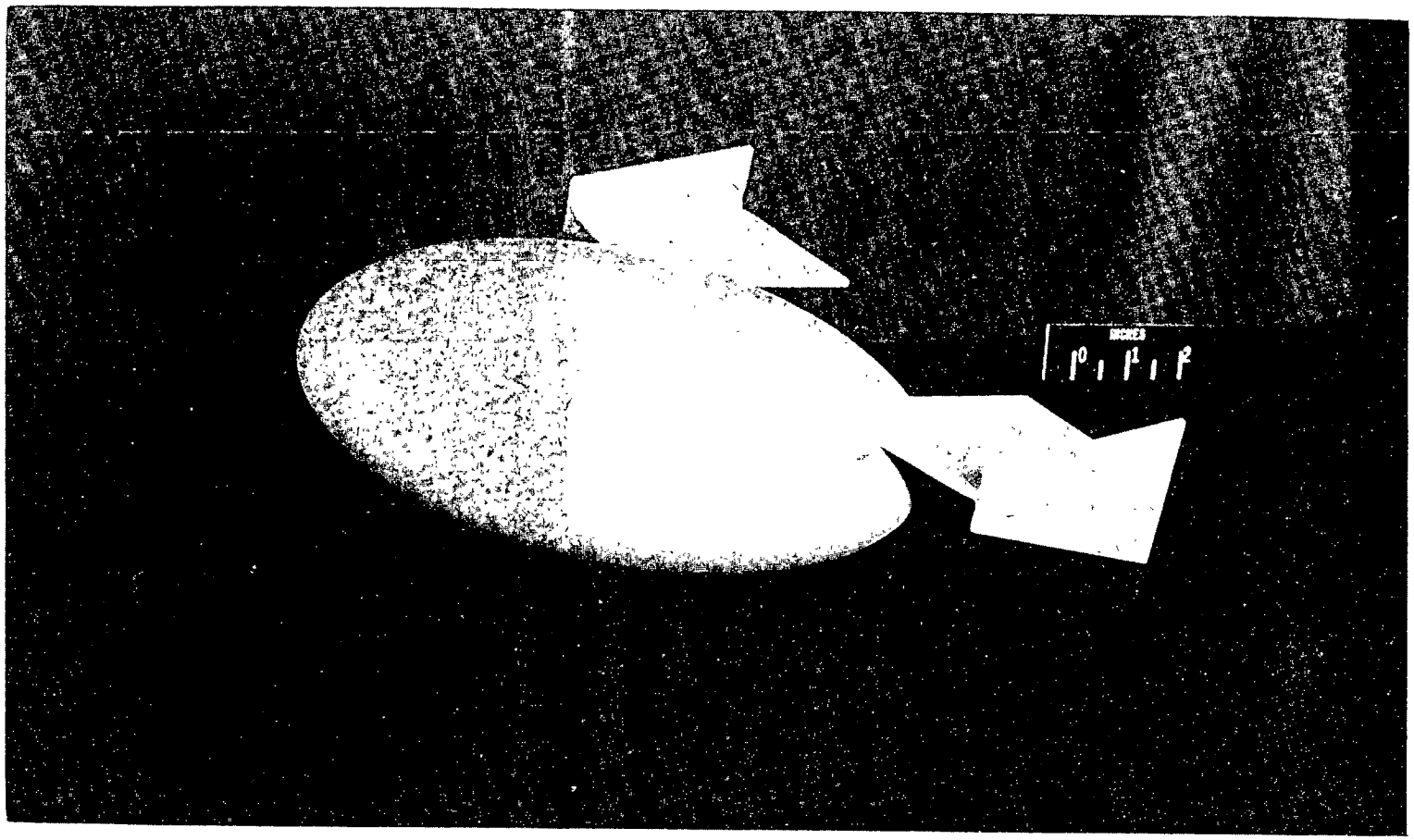

Figure 1.- Photograph of model with modified fins. L-60-753

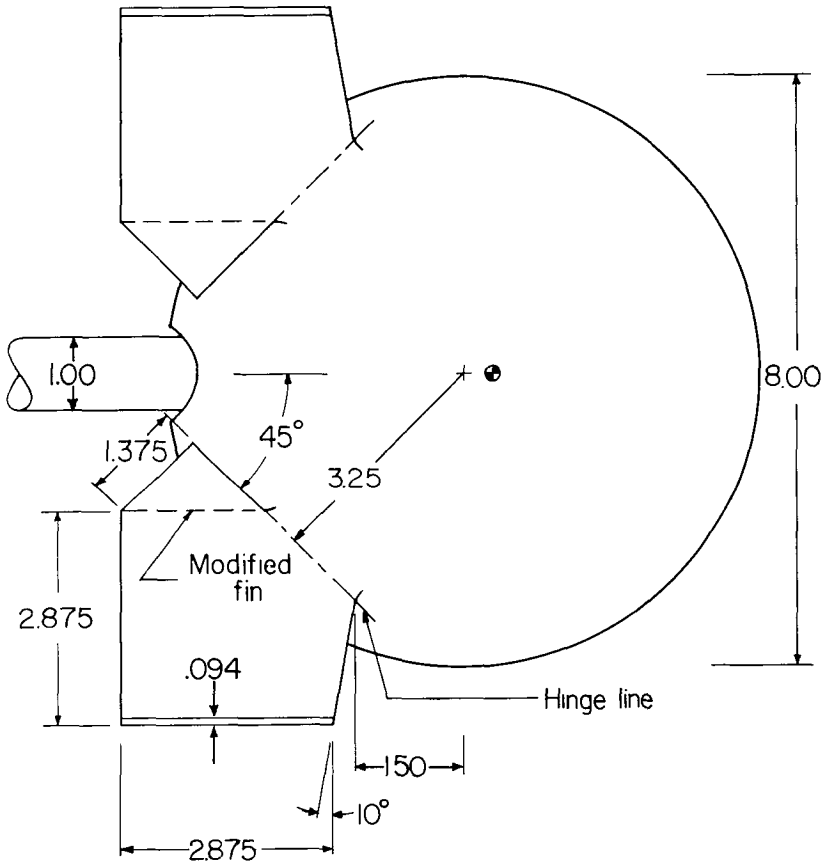

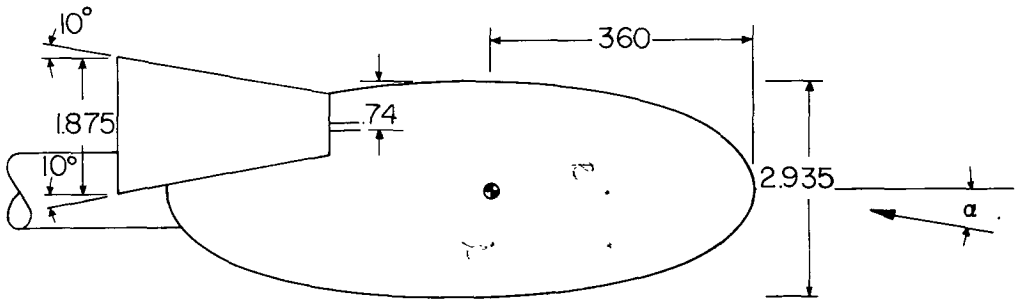

Figure 2.- Drawing of model with fins. All dimensions are in inches.

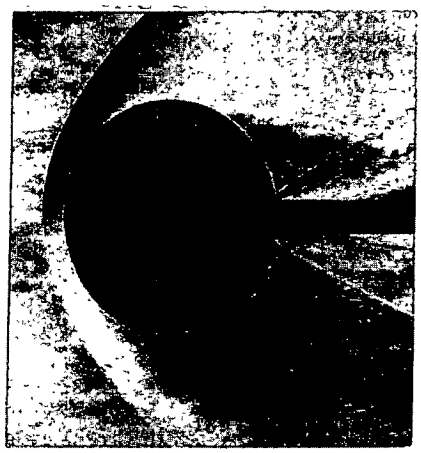

Fins off

$\alpha = 30°$

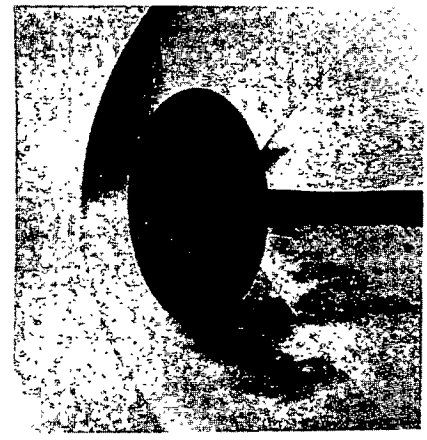

Fins off

$\alpha = 60°$

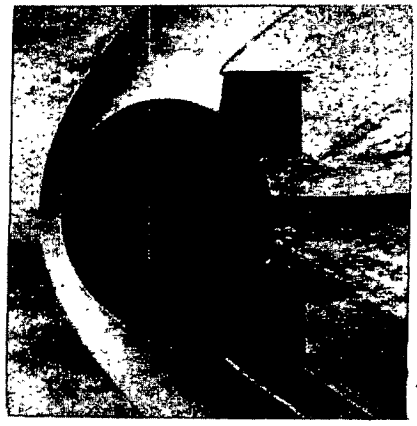

Modified fins

$\alpha = 30°$

$\delta = 0°$

Modified fins

$\alpha = 60°$

$\delta = 0°$

L-60-2488

Figure 3.- Schlieren photographs of model. M = 1.99.

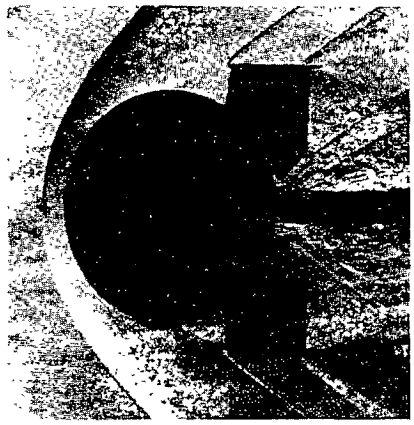

Basic fins

$\alpha = 30°$

$\delta = 0°$

Basic fins

$\alpha = 60°$

$\delta = 0°$

Basic fins

$\alpha = 30°$

$\delta = -20°$

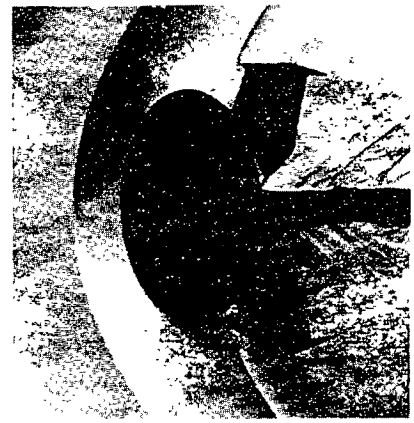

Basic fins

$\alpha = 60°$

$\delta = -20°$

Figure 3.- Concluded. L-60-2489

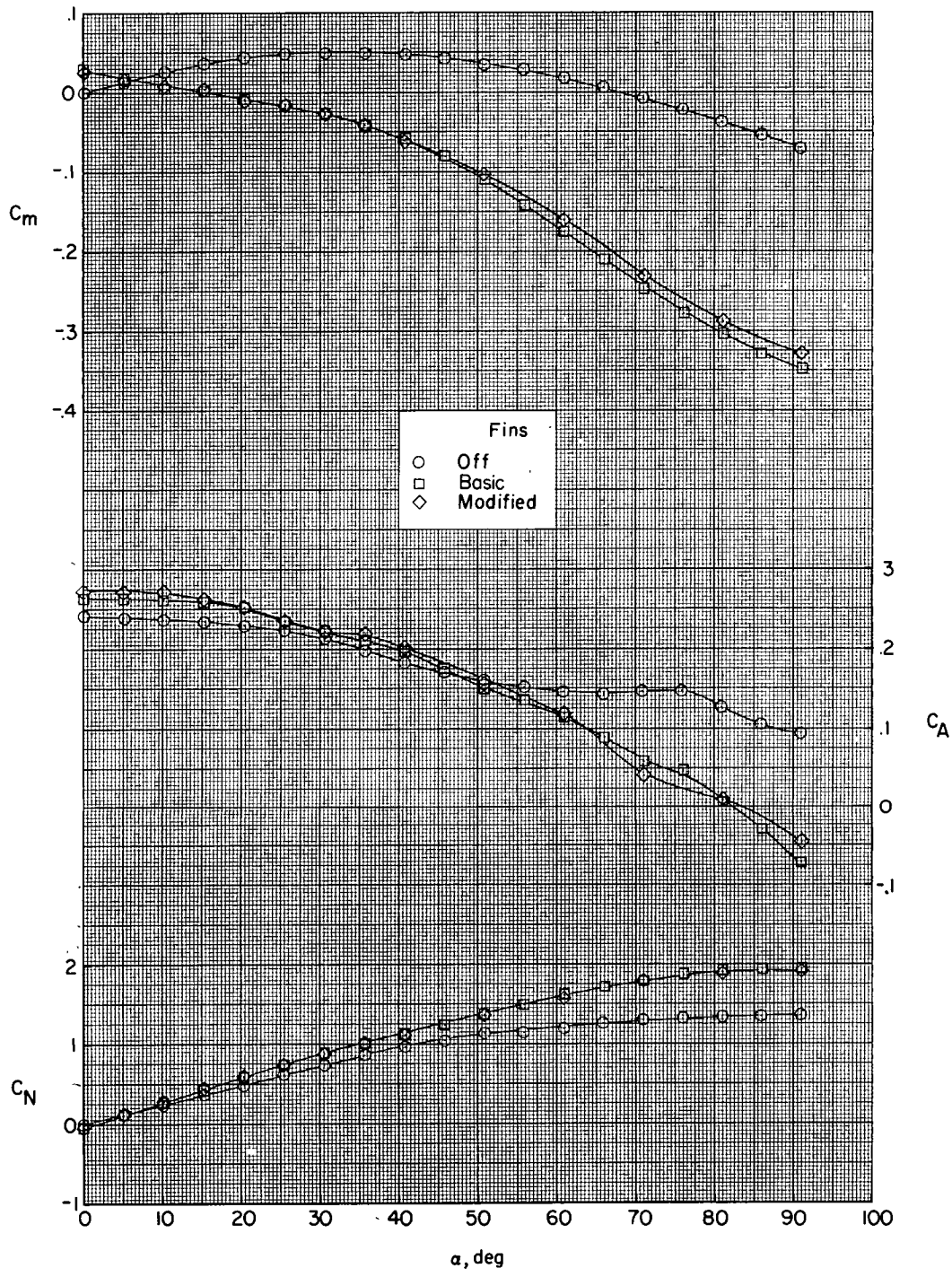

Figure 4.- Longitudinal aerodynamic characteristics of the model with fins off, basic fins, and modified fins.

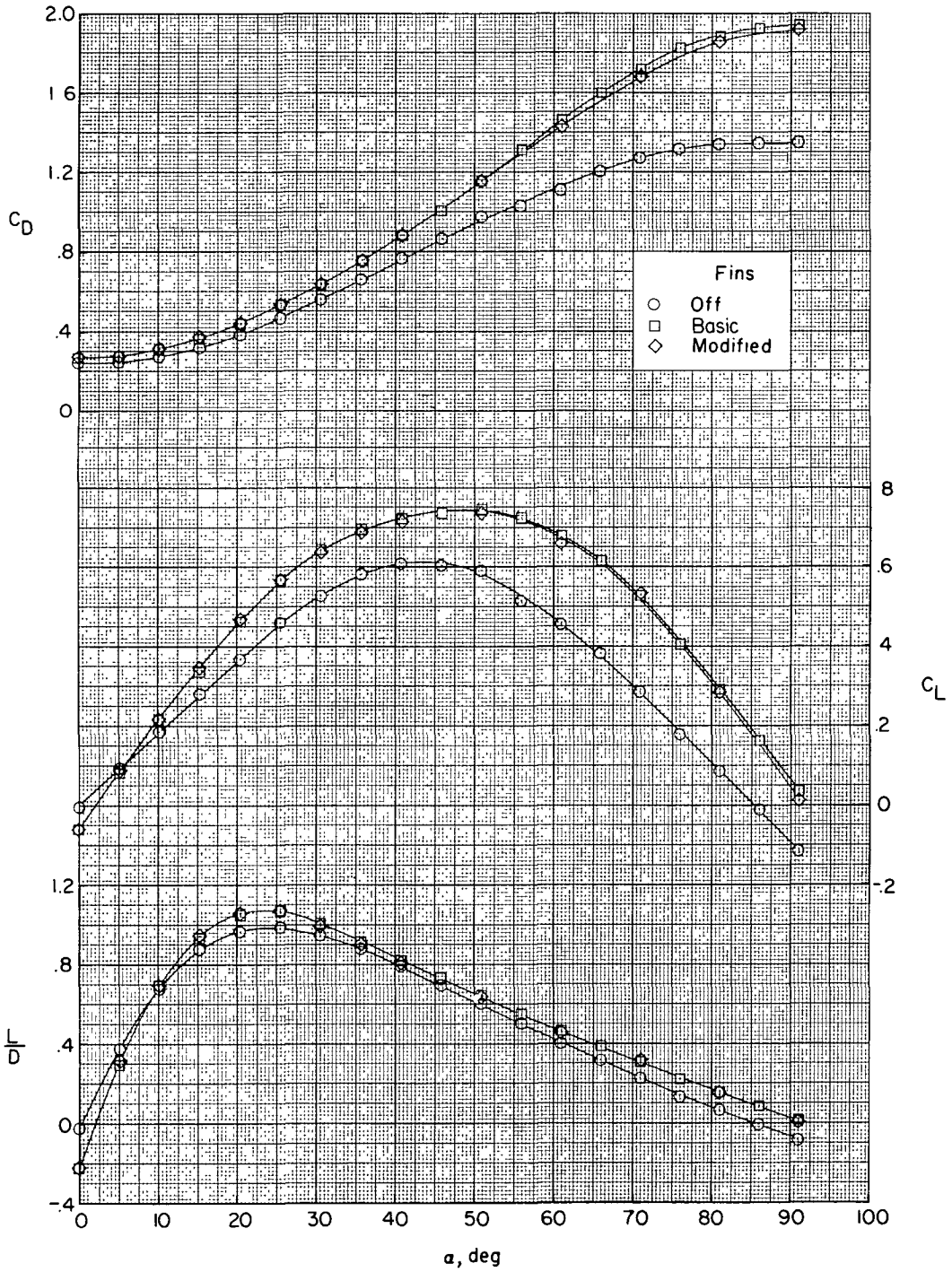

Figure 4.- Concluded.

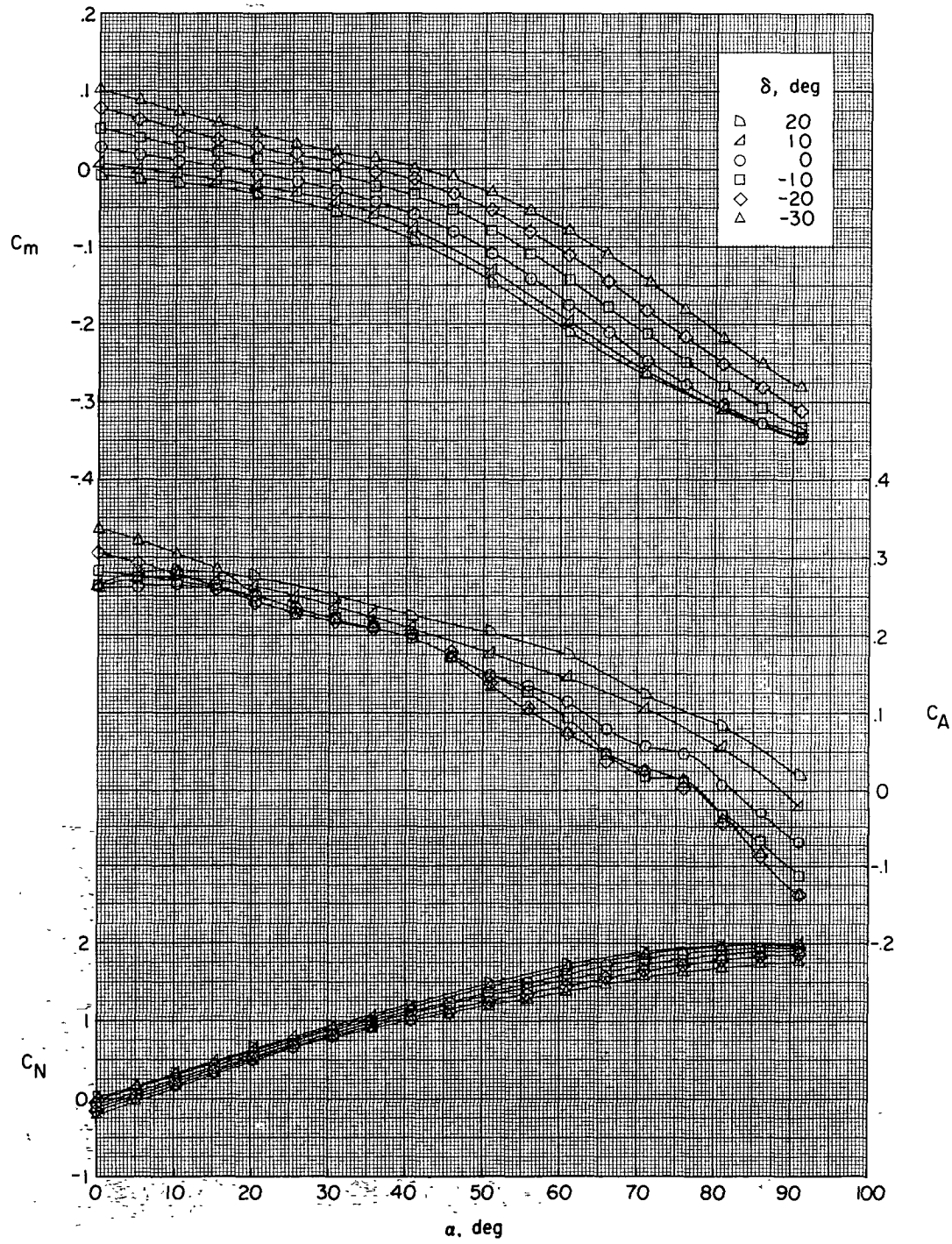

Figure 5.- Longitudinal aerodynamic characteristics of the model with basic fins at various fin deflection angles.

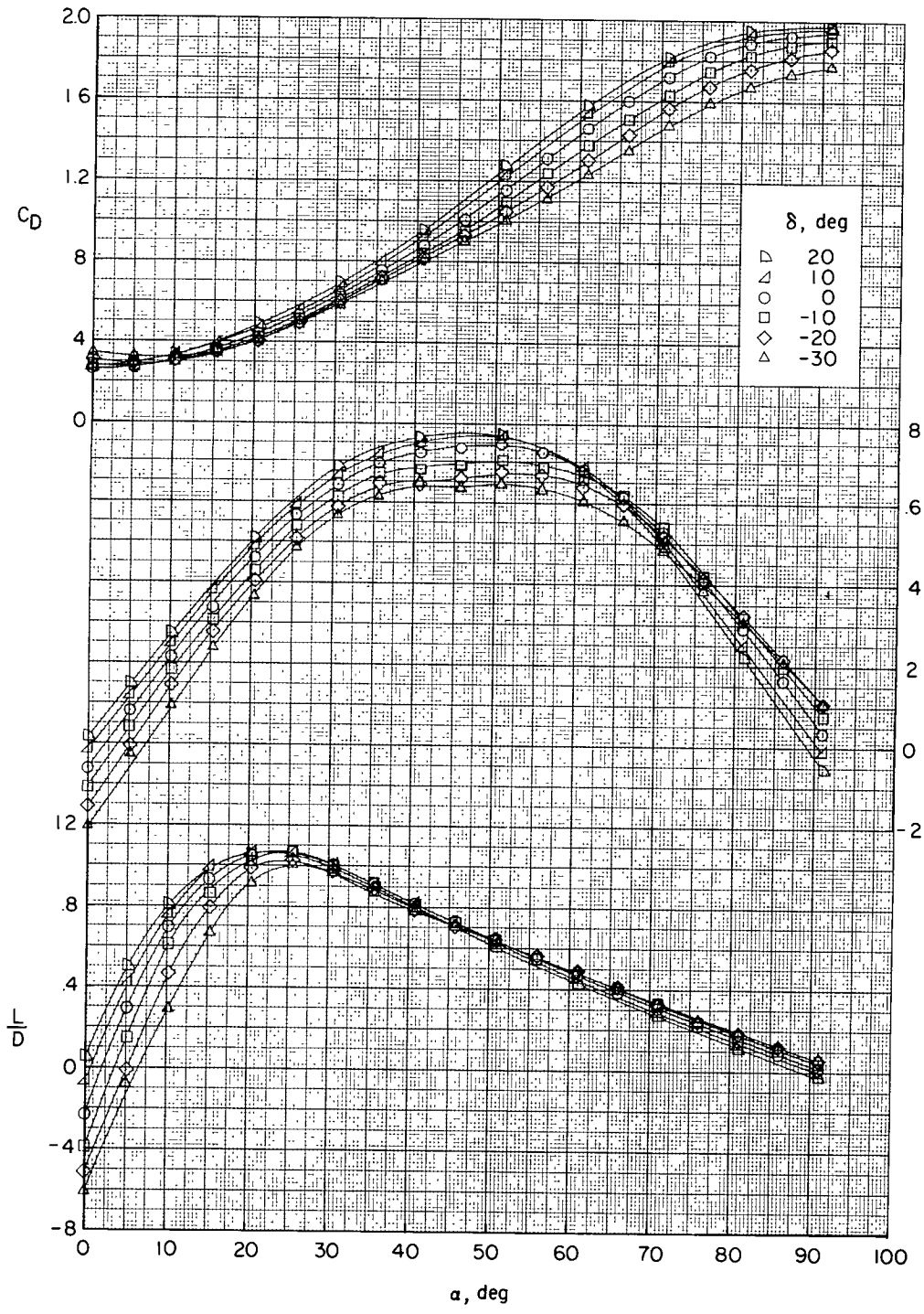

Figure 5.- Concluded.

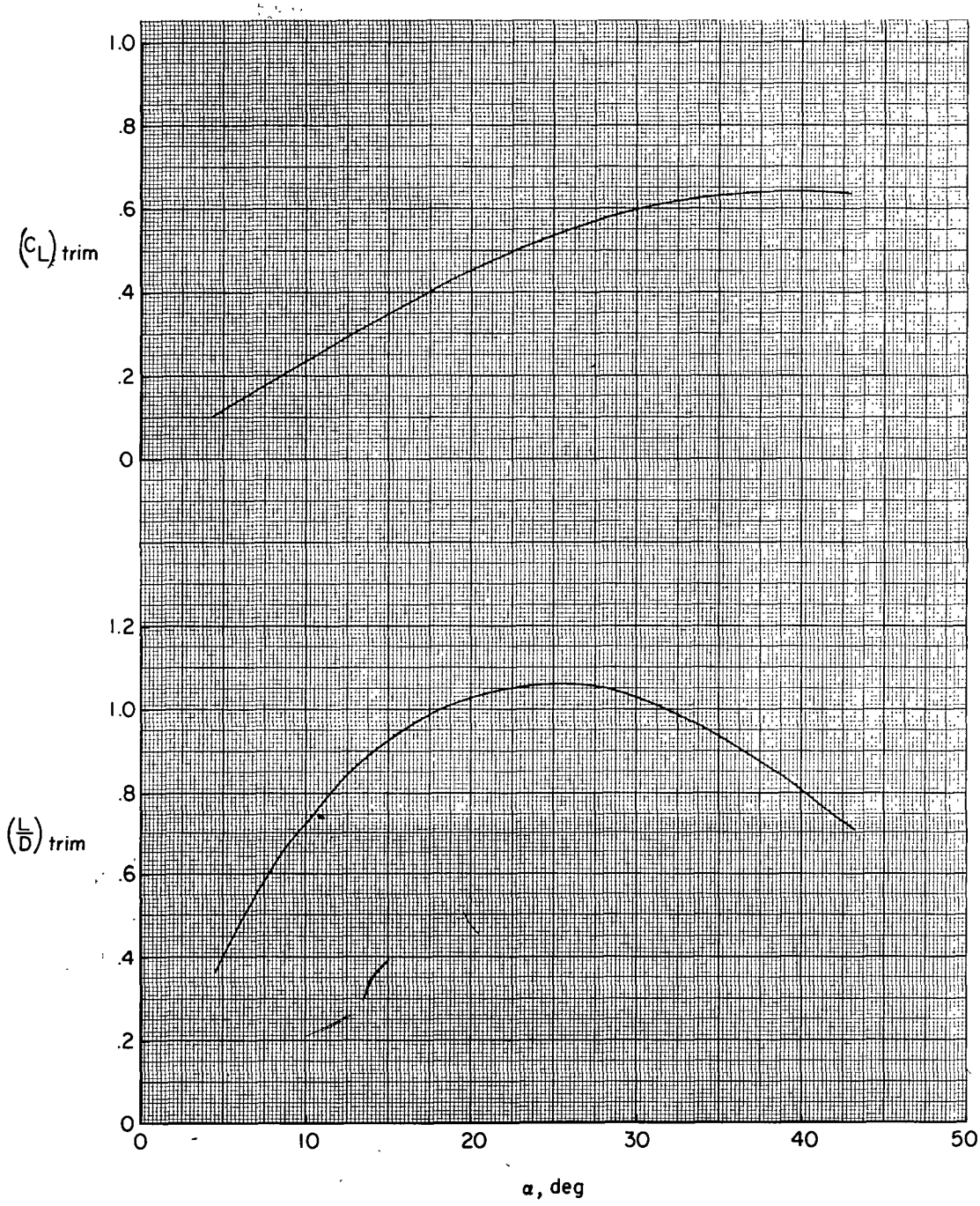

Figure 6.- Variation of $\left(\frac{L}{D}\right)_{trim}$ and $(C_L)_{trim}$ with α for the model with basic fins.

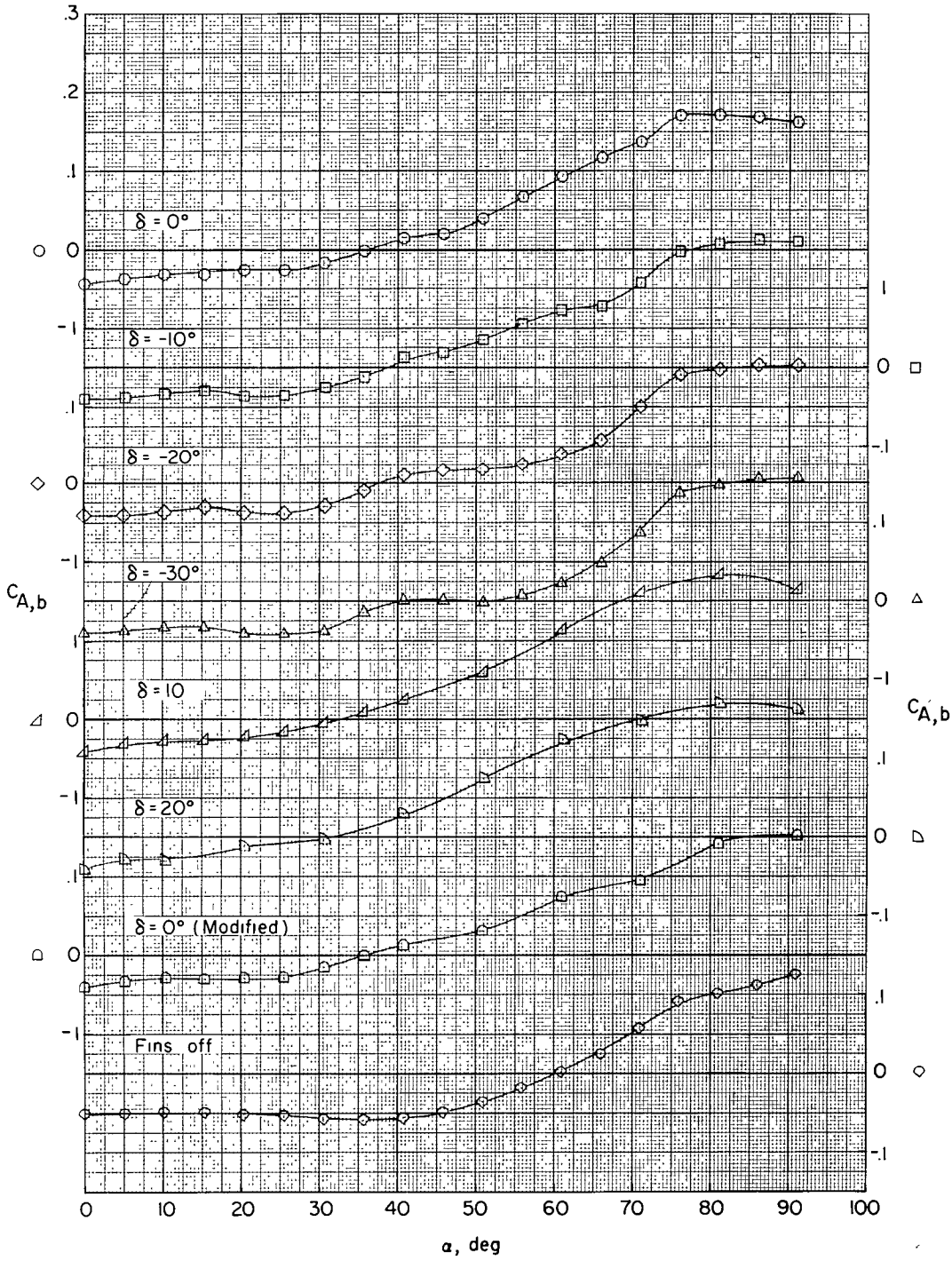

Figure 7.- Axial-force coefficients due to base pressures.